

## Original Article

# Intraoperative diagnosis of thyroid diseases by fourier transform infrared spectroscopy based on support vector machine

Min Wu, Weitao Zhang, Peirong Tian, Xiaofeng Ling, Zhi Xu

*Department of General Surgery, Peking University Third Hospital, Beijing, China*

Received September 28, 2015; Accepted January 7, 2016; Epub February 15, 2016; Published February 29, 2016

**Abstract:** Background: The recent development of attenuated total internal reflection- Fourier transform infrared (ATR-FTIR) spectroscopy has provided a new avenue for distinguishing cancerous tissue from normal one. The focus of this investigation is to develop a novel spectral discriminant method for thyroid malignant and benign samples, intraoperatively. Methods: A total of 112 cases of human thyroid tissues, were obtained and underwent ATR-FTIR spectroscopy scanning intra-operatively. The average ATR-FTIR spectra of nodular goiter and thyroid carcinoma was built. Standard normal variate (SNV) method was applied to cut down scatter effect, and support vector machine (SVM) discrimination model was used to discriminate spectra of benign thyroid diseases from malignant one. Leave-one-out cross validation (LOOCV) was exploited to evaluate SVM discriminant effects. Results: 67 nodular goiter (benign) and 45 thyroid carcinoma (malignant) were pathologically diagnosed. The average ATR-FTIR spectra of nodular goiter was significantly different from thyroid carcinoma group. The sensitivity, specificity, and accuracy rate of the SVM algorithm's discriminants were 84.4%, 88.0%, and 86.6%, respectively. Conclusion: A novel approach to distinguish nodular goiter from thyroid carcinoma intraoperatively by using the ATR-FTIR technique combined with mathematical procedures of SVM, was established and demonstrated.

**Keywords:** ATR-FTIR, SVM, discrimination, malignant, benign, thyroid diseases

## Introduction

Thyroid nodule is one of the most common physical signs indicating thyroid diseases, whether malignant or benign diseases, especially in the cases of women [1]. It is manifested that thyroid cancer shows up as a solitary thyroid nodule in 95% of cases [2]. Early and accurate diagnosis of malignant and benign thyroid diseases, which is closely associated with corresponding treatment and prognosis, is obviously extremely important. While currently, the preoperative diagnostic methods mainly include ultrasonography, computed tomography, and thyroid scanning. But the above methods have several disadvantages such as depending largely on pathologists' judgments, complicated procedures and expensive instruments. Hence it is very urgent to develop a simple and rapid method for diagnosing thyroid diseases at the early stage. Current widely practiced intraoperative methods for rapidly assessing thyroid tissues status include frozen-section and touch imprint cytology [3]. However,

these approaches have a number of disadvantages including being labor intensive, time-consuming and having variable sensitivity. Frozen-sectioning and analysis of the samples require a skilled histopathology technician and a dedicated pathologist for each surgical procedure. Therefore, intensive attention should be played on seeking an alternative method that can improve the efficiency and accuracy to differentiate between benign and malignant thyroid diseases.

An attenuated total internal reflection-Fourier transform infrared (ATR-FTIR) technique, with the absorption of electromagnetic radiation in the middle infrared range, is one of the latest and least expensive techniques used to study the structure and quantity of biochemical materials such as nuclear acids, proteins, carbohydrates, lipids [4]. In addition, cells undergo dramatic changes in biomolecules' expression and structural abnormality, such as nuclear acids, proteins, during the onset and progression of cancer. As FTIR spectroscopy can reveal bio-

# Intraoperative diagnosis of thyroid tumor using FTIR spectroscopy

**Table 1.** Clinical characteristics of 112 patients with thyroid diseases

Patients characteristics	Mean age $\pm$ SD	Sex		Diagnosis
		Male (n)	Female (n)	
Thyroid carcinoma	45.46 $\pm$ 10.25	14	31	Papillary thyroid carcinoma
Nodular goiter	51.49 $\pm$ 14.20	11	56	Thyroid adenoma

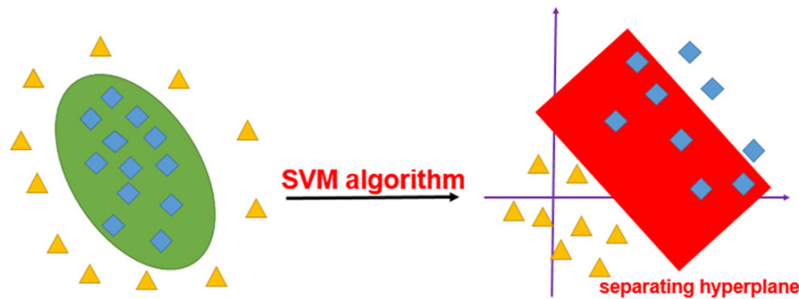


**Figure 1.** The fundamental mechanism of the discriminant analysis SVM algorithm.

chemical changes in diseased tissues and cells [5], it has been used to study gastric cancer [6], cervical cancer [7], esophageal cancer [8], gallbladder cancer [9] in recent years. It has also been applied to thyroid diseases research [10]. For example, FTIR spectroscopy coupled with Fisher's discriminant analysis was used to distinguish normal healthy, benign and malignant thyroid nodules before surgery through the subjects' skin and the result shows that the method has achieved a high discriminant accuracy of 88.8% in our previous research work [11]. Therefore, FTIR spectroscopy can be used to detect all of above changes in tissues at the molecular level and then help the surgeons to obtain prompt and accurate diagnosis.

The aim of this investigation is to develop a novel and accurate diagnostic approach-ATR-FTIR technique to differentiate malignancy from benign thyroid tissues. Specific emphasis will be placed on discriminating spectra between malignant and benign samples, by applying support vector machine (SVM) classification. The results of the SVM classification were compared with those of frozen-section examination and the final pathological diagnosis.

## Materials and methods

### Samples

A total of 112 cases with thyroid nodules underwent surgery in Peking University Third Hospital

during February, 2013 to March, 2015. The average age of these patients was  $48 \pm 12$  year old (**Table 1**). Their preliminary diagnoses were made mostly based on detailed history taking, thorough physical examination of thyroid, and various corresponding examinations including serology, biomedical tests, and especially the findings of ultrasonography. Samples were obtained from the center of the thyroid lesions during operation, and were cut into cubes (1.0 cm  $\times$  1.0 cm  $\times$  0.5 cm) and placed on ATR detection plate attached to FTIR spectro-

scopic scanning apparatus in the shortest possible time. Then samples were processed as paraffin embedded blocks for pathologic diagnosis. 67 patients were diagnosed as nodular goiter and the others as thyroid carcinoma pathologically. This study was approved by Peking University Bio-medical Ethics Committee and Institutional Review Board of Peking University Third Hospital (IRB00001052-11034) and written informed consent was obtained from each participant.

### Instrumentation

Samples were measured using attenuated total reflection (ATR) equipped with a liquid-nitrogen-cooled mercury cadmium telluride detector (Fourier transform infrared spectrometer, WQF-660, Beijing Rayleigh Analytical Instrument Co., Ltd, Beijing, China). Mid-infrared radiation was passed to and from the ATR accessory. Spectra were measured at a resolution of  $8 \text{ cm}^{-1}$ , and 32 scans were combined to achieve an acceptable signal-to-noise ratio, with wave number ranging from 1900 to  $1050 \text{ cm}^{-1}$ . Background signal was averaged over 32 scans prior to each measurement and was subtracted from sample spectrum automatically to eliminate atmospheric effects. Collection of each spectrum usually took around 2 min.

### Data analysis

A total of 112 spectra were obtained. The peak position and intensity of each band were mea-

**Table 2.** Preliminary assignments of characteristic bands of FTIR spectra of thyroid samples

Peak position (cm <sup>-1</sup> )	Vibrations of the groups	Reference substances
1640	Amide I band	Protein
1550	Amide II band	Protein
1460	δC-H	Lipid
1400	δC-H, δC-O-H	Lipid
1250	v <sub>as</sub> PO <sub>2</sub> <sup>-</sup>	Nucleic acid
1160	vC-O, δC-O-H, δC-O-C	Carbohydrate
1080	v <sub>s</sub> PO <sub>2</sub> <sup>-</sup>	Nucleic acid

v<sub>as</sub>, asymmetric stretching vibration; v<sub>s</sub>, symmetric stretching vibration δ, bending vibration.

sured using SpaPro version 2.2 software (College of Chemistry and Molecular Engineering, Peking University, Beijing, China). FTIR parameters of nodular goiter (benign) and thyroid carcinoma (malignant) were compared. Tests of normal distribution and variance of homogeneity were performed for all parameters. Normally distributed data were analyzed with Student's *t* test. The ROC analysis has also been conducted to get the sensitivity, specificity, AUC. SPSS version 20 software (IBM, Armonk, New York, USA) was used for these statistical analyses. The pre-processing steps, which included analysis and model construction, and support vector machine (SVM) classification were taken in MATLAB R2013a (MathWorks, Inc., Natick, Mass., USA). With the purpose of weakening the effect to the accuracy of modeling from the differences of sample shape, size, density and nonspecific scatter at the surface of the samples, standard normal variate (SNV) method was adopted in the analysis [12]. Each spectra was preprocessed by SNV, the spectroscopic data of sample *i* at wavenumber *k* could be standard normalized as (1):

$$x_{ik,SNV} = \frac{x_{i,k} - \bar{x}_i}{\sqrt{\sum_{k=1}^p (x_{i,k} - \bar{x}_i)^2}} (p-1)^{1/2} \quad (1)$$

Where  $\bar{x}_i$  means the average of spectroscopic data of sample *i*, while *p* is the number of the wavelength, and (*p*-1) is the freedom degrees.

Then the discriminant analysis SVM algorithm, which employs a non-linear mapping to transform the original training data into higher dimensional data and searches for the linear optimal separating hyperplane within this new

dimension, as is shown in **Figure 1**, was carried out to distinguish benign thyroid tissue from thyroid cancer [13]. The principle is explained as follows [14].

For labeled training data of the form  $(x_i, y_i) i \in \{1, \dots, n\}$ , where  $x_i$  is an *n*-dimensional.

Feature vector and  $y \in \{-1, 1\}$  the labels, a decision function is found representing a separating hyperplane defined as (2):

$$f(x) = (\langle \omega, \phi(x) \rangle + b) \quad (2)$$

where  $\omega$  is the weight vector, *b* is the bias value, and  $\phi(x)$  is the kernel function.

By projecting the data using a mapping  $\phi(x)$ , nonlinear decision boundaries in the input data space can be obtained. The separating hyperplane is found by maximizing distances to its closest data points, embedding it in a large margin which is defined by support vectors, as is shown in **Figure 1**. Finding the hyperplane while maximizing the margin is formulated as the following optimization problem:

$$\min \frac{1}{2} \omega^T \omega + C \sum_{i=1}^N \xi_i$$

subject to:  $y_i (\langle \omega, \phi(x_i) \rangle + b) \geq 1 - \xi_i$ , (3)

$$\xi_i \geq 0, (i = 1, \dots, N)$$

where *C* is the cost parameter constant,  $\xi_i$  is parameter for handling non-separable data, and the index *i* labels the *N* training cases. Note that  $y \in \{-1, 1\}$  is the class labels, and  $x_i$  is the independent variables.

Nonlinear classification using the Gaussian kernel as following equation (4) was investigated:

$$K(x, x_i) = \exp\left(-\frac{\|x - x_i\|^2}{\sigma}\right) \quad (4)$$

where  $\sigma$  is the kernel width, which controls the amount of the local influence of support vectors on the decision boundary.

For the sake of testing the efficiency of SVM algorithm, five parameters, including sensitivity, specificity, accuracy, positive predictive value and negative predictive value, were calculated for ATR-FTIR data. Leave-one-out cross Validation (LOOCV), which attempts to predict the data of the unknown sample with the data of training sample set, was employed to evaluate the discriminating power of SVM method. The results of pathological diagnosis served as

## Intraoperative diagnosis of thyroid tumor using FTIR spectroscopy

**Table 3.** FTIR spectra comparisons between nodular goiter and thyroid carcinoma

Peak Intensities	Thyroid carcinoma		Nodular goiter		Statistical t-tests	P
	N	Mean ± SD	N	Mean ± SD		
I1640	45	0.43±0.06	67	0.42±0.04	0.928	0.355
I1550	45	0.23±0.05	67	0.22±0.05	0.847	0.399
I1460	45	0.14±0.04	67	0.13±0.03	2.784	0.007*
I1400	45	0.15±0.04	67	0.13±0.03	2.621	0.011*
I1250	45	0.14±0.04	67	0.12±0.03	2.602	0.011*
I1160	45	0.13±0.04	67	0.10±0.02	3.392	0.001*
I1080	45	0.15±0.01	67	0.12±0.03	2.543	0.013*

I: the peak intensity; \*indicates that  $P < 0.05$ .

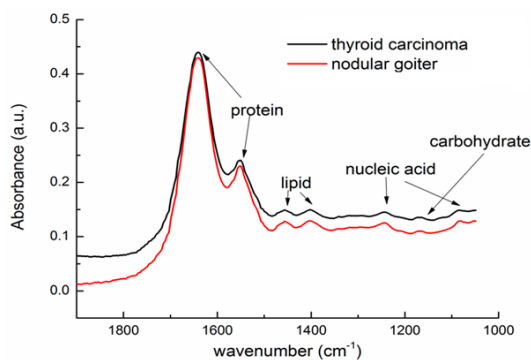


**Figure 2.** Average FTIR spectra of nodular goiter (benign) and thyroid carcinoma (malignant) with wavenumber ranging from 1050 to 1900  $\text{cm}^{-1}$ .

standard, and were compared with findings of frozen-section examination and the classification from the SVM. In all instances  $P < 0.050$  was considered statistically significant.

### Results

#### Pathological findings

Thyroid samples were fixed and sent to pathologists for diagnosis immediately after ATR-FTIR spectroscopy scanning. 67 nodular goiter (benign) and 45 thyroid carcinoma (malignant) were pathologically diagnosed, as summarized in **Table 1**. The accuracy of intraoperative frozen-section diagnosis was 100 percent.

#### ATR- FTIR spectra features of samples

Seven peaks were identified and given a preliminary assignment as nucleic acid, protein, lipid or carbohydrate in **Table 2**. Significant differences between nodular goiter and thyroid carcinoma tissues are shown **Table 3**. The para-

eters with a significant difference between the two groups were: peak positions' intensity I1460 and I1400 (related to lipid), I1240 and I1080 (related to nucleic acid), and I1160 (related to carbohydrate). However, no single parameter change could sufficiently distinguish the two groups by itself. Therefore, a single parameter could not be used as a marker to detect malignancy. **Figure 2** shows the average FTIR spectra of nodular goiter (benign) and thyroid carcinoma (malignant).

#### Discriminant analysis

Discriminant model was developed to discriminate nodular goiter (benign) from thyroid carcinoma (malignant) and LOOCV was utilized to evaluate the efficiency of SVM model. Contrast between FTIR spectroscopy technique and the standard pathologic diagnosis is presented in **Table 4**. ROC analysis indicates that the sensitivity, specificity, positive predictive value, negative predictive value and accuracy of SVM method are 84.4%, 88.0%, 82.6%, 89.3% and 86.6%, respectively. The ROC curve is presented in **Figure 3**. The original FTIR spectra of thyroid carcinoma (malignant) and nodular goiter (benign) samples and the same spectra after preprocessing of standard normal variate (SNV) are shown in **Figure 4**, in which the differences between FTIR spectra of benign and malignant tissues become pronounced, and the boundary of two clusters is clearer.

### Discussion

In order to monitor and characterize the spectral properties of benign and malignant tumor cells, various spectroscopy techniques are applied, including X-ray photoelectron spectroscopy [15], micro-spectroscopy [16], Raman spectroscopy [17] and Fourier transmission infrared spectroscopy [18]. FTIR spectroscopy, which is dependent on infrared radiation passing through a thin sample with photons of specific wavelengths being absorbed by specific functional groups, is a well-established technique to examine and visualize multi-components in the field of view [19]. When equipped

## Intraoperative diagnosis of thyroid tumor using FTIR spectroscopy

**Table 4.** Discrimination diagnosis between spectroscopy with SVM method and pathology

Diagnosis of FTIR spectroscopy with SVM method	Pathological diagnosis		Sum
	Thyroid cancer	Nodular goiter	
Thyroid cancer	38	8	46
Nodular goiter	7	59	66
Sum	45	67	112

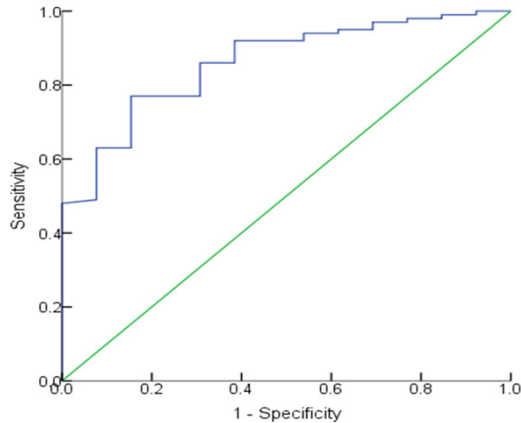


**Figure 3.** ROC analysis result of SVM method: the value of AUC is 0.866, 95% CI [0.768, 0.953],  $P < 0.000$ .

with an attenuated total internal reflection element, a series of FTIR-related problems, especially sample thickness, could be resolved, perfectly. ATR-FTIR spectroscopy is increasingly popular because of the facts that sample preparation is barely required, the inherent surface sensitivity allows highly absorbing samples to be studied and, above all, the optical path length is typically independent of sample thickness [20, 21].

As is known, human biological tissues' main constituents of substances are DNA/RNA, proteins, carbohydrates and lipids; while previous researches indicate that these bio-substances could be characterized by distinct vibrational absorption features in the ATR-FTIR spectral region, as is shown in **Table 2** [22]. When affected by pathogenic factors, such as radioactive and arsenic substance, serious pathological changes may occur in tissues, which firstly show up as variations at the molecular level and could affect the biochemical substances' compositions of biological entities, afterwards [23]. While FTIR spectroscopy could differentiate cells or tissues based on their characteristic spectral properties, which reflect

the biochemical substances' composition and structure in cells, and peak intensity level can be measure the relative content of a bio-molecule, roughly. As we can know in **Table 3** and **Figure 2**, the peak intensity that presents the nucleic acid 11250 is significantly higher in thyroid carcinoma than nodular goiter, indicative of enhanced cell proliferation in the malignant tissue, with more nucleic acid produced and also released during cell necrosis or apoptosis. Similarly, the peak intensity 11640, 11550, 11460, 11400, 11160 and 11080 are distinctly were increased in thyroid carcinoma tissues, meaning that more protein, lipid and carbohydrate was contained in the malignant tissue, which is likely to result from a faster cell metabolism.

In our study, the results obtained from applying ATR-FTIR spectroscopy combined with support vector machine method to analyze the real-time infrared spectral data of thyroid tissues intra-operatively, show that, the sensitivity, specificity, and accuracy were all high, indicating that this technique has the potential to distinguish nodular goiter from thyroid carcinoma. The accuracy of intraoperative frozen-section diagnosis in the present cohort was 100 percent. However, the results vary greatly in the literature, with sensitivity ranging from 66 to 68.8 percent, specificity from 99 to 100 percent [24, 25]. Although frozen section examination is a vital tool to the surgeons for determining whether to undertake the further radical surgery operation, it has several limitations. Above all, the consequence of intraoperative frozen section diagnosis is usually unstable and errors like the delayed diagnosis or misdiagnosis often occur due to the rush time, the finite capacity of pathologists, which even leads directly to a major controversy that whether should determine the reasonable resection range according to intraoperative frozen section [26-28]. Moreover, even fast frozen section examination generally takes about 30 minutes, which is relatively longer than the time that a total thyroidectomy actually need and may further prolong the time of surgery and anesthesia. Last, but far from least, pathological diagnosis is an invasive examination, which would destroy the samples permanently and irreversibly.

In contrast, the ATR-FTIR spectroscopy owns the nature of efficiency, only with the samples mounted on detecting device immediately with-

## Intraoperative diagnosis of thyroid tumor using FTIR spectroscopy

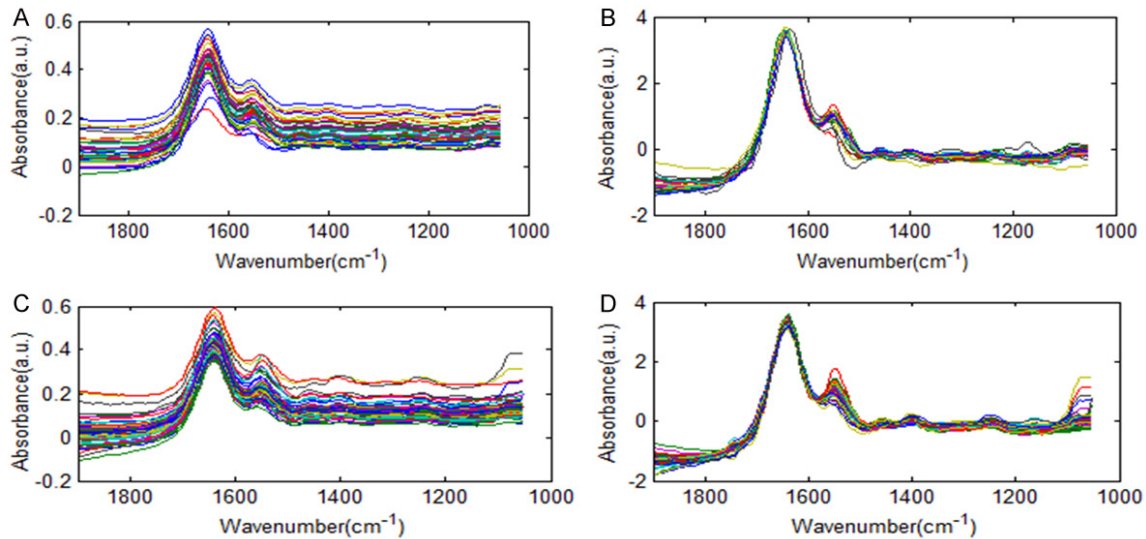


**Figure 4.** Infrared spectra of the thyroid samples: A: The original FTIR spectra of malignant; B: Malignant spectra after standard normal variate (SNV) spectra preprocessing; C: The original FTIR spectra of benign; D: Benign spectra after standard normal variate (SNV) spectra preprocessing. a.u., arbitrary units.

out no special pretreatment and this procedure taking about 2 min. Meanwhile, another advantage of ATR-FTIR spectroscopy is that it can save human from the complicated clinical work, because of that ATR-FTIR spectroscopy is simply based on spectral parameters related to the biochemical structural changes at the molecular level and calculated by a computer automatically. Besides, ATR-FTIR spectroscopy combined with SVM method is an objective rather than subjective procedure, which could exclude mistakes made by human. Since SVM is one of the machine learning algorithms based on statistic theory, it has unique advantages in solving small sample, non-linear and high dimension mode pattern discrimination. And it could build a set of hyperplanes in a high dimensional space by the pre-selected nonlinear mapping, which can be used for classification and regression [29]. With appropriate non-linear mapping to a sufficiently high dimension, a decision boundary can separate data into two clusters. It has been said that SVM could compensate the influence of uncertainty and nonlinearity in spectral quantitative analysis due to its high accuracy and good generalization ability [30]. Therefore, ATR-FTIR spectroscopy combined with SVM discrimination system may have the potential to offer a new, safe and effective alternative in the diagnosis of classifying nodular goiter from thyroid carcinoma and helping physicians to avoid unnecessary mistakes. With the development of further ATR-FTIR tech-

nology and deeper improvement of tumor understanding, we believe that this technique will soon turn out to be a routine screening tool to stage and grade the tumors in clinic setting and help surgeons solving their most stressing problems like how to make rapid diagnosis, decide the extent of surgical dissection and avoid unnecessary tissue resection in surgery.

### Conclusions

A novel approach to distinguish nodular goiter from thyroid carcinoma by using the ATR-FTIR technique combined with mathematical procedures of SVM, was established and demonstrated. The results of this study show that its accuracy rate can reach up to 86.6 percent. It is anticipated that the ATR-FTIR combined with SVM approach turns out to be a useful diagnostic tool in clinic.

### Acknowledgements

The authors would like to acknowledge the Beijing Natural Science Foundation and Peking University Third Hospital for giving grants.

### Disclosure of conflict of interest

None.

**Address correspondence to:** Dr. Zhi Xu, Department of General Surgery, Peking University Third

# Intraoperative diagnosis of thyroid tumor using FTIR spectroscopy

Hospital, 49 North Garden Road, Hai-Dian District, Beijing 100191, China. Tel: +86-010-82267331; E-mail: xuzhi123456@sohu.com

## References

- [1] Bernard W. Stewart and Christopher P. Wild. World Cancer Report 2014. IARC Nonserial Publication 2014.
- [2] Lumachi F, Borsato S, Tregnaighi A, Marino F, Poletti A, Iacobone M, Favia G. Accuracy of fine-needle aspiration cytology and frozen-section examination in patients with thyroid cancer. *Biomed Pharmacother* 2004; 58: 56-60.
- [3] Weiser MR, Montgomery LL, Susnik B, Tan LK, Borgen PI, Cody HS. Is routine intraoperative frozen-section examination of sentinel lymph nodes in breast cancer worthwhile. *Ann Surg Oncol* 2000; 7: 651-655.
- [4] Sun X, Xu Y, Wu J, Zhang Y and Sun K. Detection of lung cancer tissue by attenuated total reflection-Fourier transform infrared spectroscopy-a pilot study of 60 samples. *J Surg Res* 2013; 179: 33-38.
- [5] Tian P, Zhang W, Zhao H, Lei Y, Cui L, Zhang Y, Xu Z. Intraoperative detection of sentinel lymph node metastases in breast carcinoma by Fourier transform infrared spectroscopy. *Br J Surg* 2015; 102: 1372-9.
- [6] Li Q, Wang W, Ling X, Wu JG. Detection of gastric cancer with Fourier transform infrared spectroscopy and support vector machine classification. *Biomed Res Int* 2013; 2013: 942427.
- [7] Walsh MJ, Singh MN, Pollock HM, Cooper LJ, German MJ, Stringfellow HF, Fullwood NJ, Paraskevaidis E, Martin-Hirsch PL, Martin FL. ATR microspectroscopy with multivariate analysis segregates grades of exfoliative cervical cytology. *Biochem Biophys Res Commun* 2007; 352: 213-9.
- [8] Maziak DE, Do MT, Shamji FM, Sundaresan SR, Perkins DG, Wong PT. Fourier-transform infrared spectroscopic study of characteristic molecular structure in cancer cells of esophagus: an exploratory study. *Cancer Detect Prev* 2007; 31: 244-53.
- [9] Wang J, Zhang J, Wu W, Duan X, Wang S, Zhang M, Zhou S, Mo F, Xu Y, Shi J, Wu J. Evaluation of gallbladder lipid level during carcinogenesis by an infrared spectroscopic method. *Dig Dis Sci* 2010; 55: 2670-5.
- [10] Zhang X, Xu Y, Zhang Y, Wang L, Hou C, Zhou X, Ling X, Xu Z. Intraoperative detection of thyroid carcinoma by fourier transform infrared spectrometry. *J Surg Res* 2011; 171: 650-6.
- [11] Zhang WT, Tian PR, Zhu Q, Zhang YF, Cui L, Xu Z. Noninvasive surface detection of papillary thyroid carcinoma by Fourier transform infrared spectroscopy. *Chem Res Chin Univ* 2015; 31: 198-202.
- [12] Barnes RJ, Dhanoa MS and Lister SJ. Standard normal variate transformation and de-trending of near-infrared diffuse reflectance spectra. *Appl Spectrosc* 1989; 43: 772.
- [13] Zhang Y, Ren J, Jiang J. Combining MLC and SVM Classifiers for Learning Based Decision Making: Analysis and Evaluations. *Comput Intell Neurosci* 2015; 2015: 423-581.
- [14] Keerthi SS, Lin CJ. Asymptotic behaviors of support vector machines with Gaussian kernel. *Neural Comput* 2003; 15: 1667-89.
- [15] Gilbert JB, Rubner MF, Cohen RE. Depth-profiling X-ray photoelectron spectroscopy (XPS) analysis of interlayer diffusion in polyelectrolyte multilayers. *Proc Natl Acad Sci U S A* 2013; 110: 6651-6.
- [16] Happillon T, Untereiner V, Beljebbar A, Gobinet C, Daliphard S, Cornillet-Lefebvre P, Quinquenel A, Delmer A, Troussard X, Klossa J, Manfait M. Diagnosis approach of chronic lymphocytic leukemia on unstained blood smears using Raman microspectroscopy and supervised classification. *Analyst* 2015; 140: 4465-72.
- [17] Xiao C, Flach CR, Marcott C, Mendelsohn R. Uncertainties in depth determination and comparison of multivariate with univariate analysis in confocal Raman studies of a laminated polymer and skin. *Appl Spectrosc* 2004; 58: 382-9.
- [18] Pezzei C, Brunner A, Bonn GK, Huck CW. Fourier transform infrared imaging analysis in discrimination studies of bladder cancer. *Analyst* 2013; 138: 5719-25.
- [19] Ling C and Sommer AJ. The Advantages of an Attenuated Total Internal Reflection Infrared Microspectroscopic Imaging Technique for the Analysis of Polymer Laminates. *Microsc Microanal* 2015; 21: 626-36.
- [20] Gulley-Stahl HJ, Bledsoe SB, Evan AP, Sommer AJ. The advantages of an attenuated total internal reflection infrared microspectroscopic imaging approach for kidney biopsy analysis. *Appl Spectrosc* 2010; 64: 15-22.
- [21] Burka EM, Curbelo R. Imaging ATR spectrometer. U.S. patent 6141100, 2000.
- [22] Mantsch HH, Chapman D. Infrared spectroscopy of biomolecules. New York: Wiley-Liss; 1996.
- [23] Fernandez DC, Bhargava R, Hewitt SM and Levin IW. Infrared spectroscopic imaging for histopathologic recognition. *Nat Biotechnol* 2005; 23: 469-474.
- [24] Jozaghi Y, Richardson K, Anand S, Mlynarek A, Hier MP, Forest VI, Sela E, Tamilia M, Caglar D, Payne RJ. Frozen section analysis and sentinel lymph node biopsy in well differentiated thyroid cancer. *J Otolaryngol Head Neck Surg* 2013; 11: 42-48.
- [25] Park YM, Wang SG, Goh JY, Shin DH, Kim IJ, Lee BJ. Intraoperative frozen section for the

## Intraoperative diagnosis of thyroid tumor using FTIR spectroscopy

- evaluation of extrathyroidal extension in papillary thyroid cancer. *World J Surg* 2015; 39: 187-93.
- [26] McHenry CR, Raeburn C, Strickland T, Marty JJ. The utility of routine frozen section examination for intraoperative diagnosis of thyroid cancer. *Am J Surg* 1996; 172: 658.
- [27] Butler-Henderson K, Lee AH, Price RI and Waring K. Intraoperative assessment of margins in breast conserving therapy: a systematic review. *Breast* 2014; 23: 112-119.
- [28] Cetin B, Aslan S, Hatiboglu C, Babacan B, Onder A, Celik A, Cetin A. Frozen section in thyroid surgery: Is it a necessity? *Can J Surg* 2004; 47: 29.
- [29] Christopher JC. A tutorial on support vector machines for pattern recognition. *Data Min Knowl Discov* 1998; 2: 121-167.
- [30] Mello C, Marangoni A, Poppi R and Noda I. Fast determination of thyroid stimulating hormone in human blood serum without chemical pre-processing by using infrared spectroscopy and least squares support vector machines. *Anal Chim Acta* 2011; 696: 47-52.